Safety and efficiency management in LGV operated warehouses

Safety and efficiency management in LGV operated warehouses ☆

Marina Raineri[1], Simone Perri[2], Corrado Guarino Lo Bianco[1,*]

Abstract

In the industrial world, physical borders between men and machines are vanishing because of the collaborative tasks imposed by the new productive methods. Clearly, this poses safety issues which were not present in classical plants. For example, safety problems naturally arise in the case of autonomously guided industrial vehicles because, for obvious service needs, they share their workspace with human coworkers: only limited physical protections can be adopted. In this context, a speed planner has been recently proposed for the management of the laser guided vehicles operating in automatic warehouses. Such planner does not only generate efficient trajectories, but it also ensures that they are safe. This work describes, after a brief survey on the safety management in automatic warehouses, the tests which were carried out for the experimental validation of the planner. Tests were first executed in a demonstration plant appositely designed and, later, in a real warehouse by considering actual operating conditions. The validation campaign in the production plant lasted several months, thus allowing the acquisition of a consistent amount of statistical data.

Keywords: Laser guided vehicles, safety management, velocity planner, jerk bounds, time efficiency, real-time.

1. Introduction

Nowadays, robotic systems are massively used in many industrial contexts because of their efficiency, robustness, and precision. For example, in automated warehouses Laser Guided Vehicles (LGV) are adopted for the transportation of huge loads. As asserted in [1], vehicles used in industrial contexts must be largely autonomous: they must localize themselves, follow the assigned path, and manage emergency situations. The localization problem is normally handled

☆This work was supported in part by the European Project ECHORD++ (The European Coordination Hub for Open Robotics Development) financed in the framework of the FP7 EU program.

*Corresponding author
Email address: guarino@ce.unipr.it (Corrado Guarino Lo Bianco)
[1]Dip. di Ingegneria e Architettura - University of Parma
[2]Elettric80 S.p.A.

by means of laser sensors, [2], even if it must be pointed out, for completeness, that alternative solutions have been proposed for indoor vehicles. For example, [3] proposes a navigation control based on magnetic guides.

Working spaces for humans and machines, which have been historically kept separate for safety reasons, progressively tend to overlap because of the use of autonomous vehicles. For example, the separation between the two worlds has almost disappeared in automatic warehouses, where coworkers directly interact with LGVs for supervision and maintenance reasons: differently from other industrial contexts, completely disjointed working spaces can not be conceived at all. In fact, in large warehouses vehicles maintenance is carried out by avoiding plant stops for productive reasons: in case of failures, human operators necessarily enter the vehicles workspace for the required restorations. Additionally, load and transport operations which can not be managed by LGVs are handled through human-operated forklifts, which naturally share the workspace with the autonomous ones.

The motion safety problem has consequently become a "hot" topic and, consequently, it has also been widely discussed by the scientific literature, [4] and [5]. Strict regulations must be followed when humans and autonomous systems share the same workspace. A classification of the possible hazard situations, and of the techniques that can be used for their management, is proposed in [6]. The survey paper classifies the known approaches into three classes on the basis of the obstacle typology and of the time horizon considered. One of the first classification methods proposed was based on the so-called "velocity obstacles" [7], subsequently reformulated in a probabilistic version in [8]. The same concept was further extended in [9], so as to consider real-time contexts and to account for multi-agent systems. A common limit for all the mentioned strategies is represented by the need of an analytical representation for positions and speeds of the moving obstacles: such requirement can be hardly met in an LGV industrial plant. Indeed, LGVs workspace is only partially structured – vehicles move between shelves, columns, and other fixed obstacles – and it is shared with several independent agents like other LGVs, human operated forklifts, temporary obstacles, and human coworkers. Obstructions along the routes occur randomly, so that they can not be analytically predicted.

An alternative method, which overcomes the limitations of the "velocity obstacles" methodologies, is based on the so called "Inevitable Collision States" (ICS). Such method assumes that mobile robots have limited sensing capabilities, so that potential obstacles are detected when their distance from sensors is below a given threshold. The ICS concept was first introduced in [10]: ICSs were formally defined and their properties were illustrated. Later, an efficient algorithm was developed [11] in order to make ICSs suitable for practical applications: indeed, the characterization of an ICS is normally difficult due to its computational complexity. ICSs have been largely studied in the literature and many works use them in order to guarantee a safe navigation. In fact, the ICS concept, which was originally conceived for the car-like model, has also been later adopted for the management of other vehicles. For example, in [12] ICSs have been reformulated in order to consider a motorcycle interacting with some

cars in a dynamic environment. The approach used for the safety management in LGV based plants can be classified among the other ICS methods. Each LGV is equipped with laser sensors which inspect a restricted area around the vehicle: a potential obstacle is revealed only when it enters the sensors field.

Working conditions in LGV plants raise serious hazard issues which are handled at different levels. First of all, rigid rules are imposed to the vehicles motion. For example, the plant layout is defined in advance and can not be modified, so that human coworkers become used of the LGVs habits and naturally tend to leave free any space which is used by the machines. Operators who need to enter zones crossed by trajectories are spontaneously inclined to pay attention. For the same reason, vehicles must never abandon the assigned trajectories, so as to avoid unexpected, and consequently dangerous, situations. This implies that, in the presence of unexpected obstacles along the route, which may be objects or coworkers, vehicles must be safely stopped in order to avoid impacts.

The safety problem is not the only one that needs to be tackled in LGV plants. In fact, in industrial contexts the productivity must be maximized and, to this purpose, velocity planners cover a central role. Generated trajectories must be minimum-time, compatibly with the assigned constraints and must be smooth, i.e., they must be jerk limited. Furthermore, it can be easily verified that the constraints fulfillment imposes variable velocity bounds: such requirement has a great impact on the planner complexity. Finally, vehicles routes are obtained by composing simple planning primitives, whose sequence is variable being defined by a supervisory system depending on the needs of the industrial plant. Vehicles receive indication of the next segment to be used shortly before the end of the current one. This implies that velocity references can not be planned in advance but, conversely, they must be evaluated in real time, depending on the typology of the assigned segment.

For all the above reasons, in LGV plants, trajectories are usually generated through the path-velocity decomposition approach initially proposed in [13] and [14]. Among the early works which adopted such method it is worth mentioning [15] and [16]. More in details, in [15] the velocity reference was obtained by accounting for the existence of kinematic and dynamic constraints. Furthermore, variable bounds were considered for the speed, but no limits were posed on the jerk. The algorithm proposed in [16] was able to plan paths and velocity references so as to avoid collisions among mobile robots. However, the driving signals were computed before the beginning of the motion for computational reasons. Many other approaches have been proposed over the years for the management of autonomous vehicles. In [17] a potential field method was used in order to obtain both the path and the velocity reference for a robot tracking a target. Nevertheless, potential fields, which are widely used in robotics, are not admissible in LGV applications since, according to the premises, vehicle paths are unmodifiable. In [18] the velocity planning was optimized by using a probabilistic prediction of the traffic-signal. The method was conceived for urban environments. In industrial plants, a predictive model can not be formulated since obstacles are revealed only at the time the vehicles need to be stopped. In [19] the velocity planning problem was reformulated in terms of a convex

optimization and the associated discretized problem was solved through a local search based on graph methods whose computational times are compatible with the real-time requirement. However, jerk limits were not accounted for and their addition would unacceptably extend the evaluation times.

The previous discussion makes it possible to evince that all mentioned velocity planners are not suited for LGV plants, bearing also in mind that they do not take into account the safety problem. The list of the potential planners is clearly not limited to the works just proposed, but similar considerations hold for all of them.

Due to the limited computational capabilities of the LGVs control units, velocity references are always obtained through computationally light algorithms. Such limitation prevents computing the velocity reference through nonlinear optimizers, since their computational times are not compatible with the real-time requirement. For this reason, the speed is normally assumed constant along each segment of the composite path: when two segments are sequentially executed, the corresponding velocities are joined by means of light-weight algorithms like, for example, the ones used for the generation of Double-S profiles [20]. Such planning strategy reduces the plant efficiency because the constant reference must necessarily coincide with the speed of the worst-case point of each segment.

The safety risks prevention and the simultaneous generation of efficient motions motivated the development of the novel velocity planner proposed in [21], which is indicated in the following as SAFERUN Algorithm (SA). The SA returns solutions which are much more efficient than the ones provided by the Standard Planner (SP) normally used in LGV plants, i.e., a planner based on the assumption of a constant speed along each segment of the composite path. In addition, the SA traveling times are comparable with the homologous ones obtained through a nonlinear solver, whose convergence times are several order of magnitude higher. Differently from other real-time solutions, the SA handles variable speed constraints by also managing acceleration and jerk limits. For the first time, safety was converted into an analytical constraint used for the synthesis of minimum-time velocity references. Hence, the planner proposed in [21] was conceived to satisfy both the real-time and the efficiency requirements, by simultaneously managing possible safety issues.

The SA is the main outcome of an experiment entitled SAFERUN (Secure And Fast rEal-time planneR for aUtoNomous vehicles) implemented in the framework of the European Project ECHORD++ (The European Coordination Hub for Open Robotics Development). The experiment explicitly contemplated a direct collaboration between University and Industry for the application of recent scientific advances in industrial contexts. In this paper, which represents the natural prosecution of [21], the planning methodology is validated on the field, i.e., in a real warehouse. The performances of the new planner are compared with the ones achieved through the SP and details will be given concerning the implementation issues.

The paper is organized as follows. Section 2 proposes a short survey on the management of the safety problems in LGV based warehouses. Section 3 reports

the experimental outcomes obtained in a demonstration plant. Proposed tests concern both the safety and the efficiency performances of the novel planner, which are compared with the homologous ones achieved with the SP. Section 4 describes an extensive test campaign executed in a real warehouse under actual operating conditions. The SA was used to replace the standard planner of two LGVs. Then, the upgraded vehicles operated with continuity in the plant together with other LGVs using the SP. A three months comparative analysis is proposed. The final discussion in Section 5 concludes the paper.

2. Safety management in LGV plants

Automated plants in which humans and machines share the same working areas may give rise to safety concerns and, consequently, they must comply with apposite rules issued by specific committees like the American ITSDF (Industrial Truck Standards Development Foundation) and the European ISO (International Standards Organization). In particular, the directives which refer to Automated Guided Vehicles (AGV) are respectively specified in the "ANSI/ITSDF B56.5-2012" document [22] for the ITSDF committee and in the two documents "EN ISO 1525:1997" [23] and "EN ISO 1526:1997+A1:2008" [24] for the ISO committee. The ANSI and the ISO guidelines are very similar: the first parts of both directives are dedicated to pose the safety requirements for automatic guided industrial vehicles, while the second ones concern automated functions for manned industrial vehicles. Such international directives pose general rules and only provide a set of guidelines to be followed. In details, both directives agree that plants must be supervised by competent technicians and trained operators who have to move carefully in the areas shared with vehicles, since hazard situations can not be avoided only by mechanical means. For what concerns the stopping distance the "ANSI/ITSDF B56.5-2012" directive states "The determination of the vehicle's stopping distance (...) depends on many factors, (...). The prime consideration is that the braking system in conjunction with the detection system and the response time of the safety control system shall cause the vehicle to stop prior to impact between the vehicle structure (...) and an obstruction (...)." The same directive also provides an exception which is at the basis of the safety management techniques used for LGVs: "Although the vehicle braking system may be performing correctly and as designed, it cannot be expected to function as designed and specified (...) should an object suddenly appear in the path of the vehicle and within the designed safe stopping distance." In practice, this implies that safety systems must be conceived to promptly react and stop vehicles in case of static obstacles, while in case of moving ones which suddenly enter the LGV workspace, the kinetic energy must be rapidly lowered, so as to minimize possible consequences. Such concept is implemented by the ASTM F3265-17 [25] directives, which propose a methodology for testing the vehicles reactions in case of detection of moving obstacles.

Standards posed by ISO and ANSI have been acknowledged by local legislations. For example, in Europe all machineries must be produced and installed

(a) (b)

Figure 1: On board safety laser sensors (yellow circles) and emergency stop devices (cyan ellipsoids) of a LGV (Courtesy of Elettric80)

.

complying with the European Machinery Directive 2006/42/EC. The same directive has been adopted by each single country of the European Community through local laws, e.g., in Italy through Legislative Decree 27.01.2010, no. 17 and through the Legislative Decree 9.04.2008, no. 81. This latter states: "If work equipment is moving in a work area, circulation rules must be established (...); Organizational measures must be taken in order to prevent workers on foot entering the area of operation of the self-propelled work equipment. If the presence of workers on foot is necessary for the proper execution of the work, appropriate measures must be taken to prevent workers from being injured by the equipment."

In order to comply with the safety directives, LGVs used in automated warehouses are equipped with certified Safety Laser Scanners (SLS), which operate similarly to standard scanners but provide a different output. Indeed, common lasers return the distances from possible obstacles measured along the directions scanned by the laser beam. Starting from such information, it is potentially possible to create a customized algorithm which reconstructs the vehicle surroundings, thus allowing a very accurate management of the safety concerns. However, any custom algorithm directly implemented by LGV manufacturers should undergo a long and expensive certification process, so that companies always adopt an alternative solution. More precisely, the market offers certified SLSs which are internally equipped with an algorithm for the safety management: users specify the areas that must be kept under control and the sensor verifies if they are free from obstacles. Practically, the sensor output is binary, i.e., the area is clear or not, while obstacle positions are not provided at all.

The advantage of this approach is that safety algorithms are directly certified by sensors manufactures, thus relieving LGV producers from any liability. The drawback of such solution is that obstacle positions are unknown: obstacles, if detected, are somewhere within the programmed safety area.

LGVs are equipped with several certified SLSs. At least four laser scanners are installed by assuming the classic configuration shown in Fig. 1: sensor 1 scans the front of the vehicle, sensor 2 is placed on its rear, while scanners 3 and 4 inspect its lateral sides. Mentioned devices are installed under the vehicle bodywork. Such position allows detecting obstacles up to an elevation roughly equal to $2 \cdot 10^{-2}$ m. Objects located over such threshold are sensed through further scanners indicated in the figure with 5 and 6, which are located on the top of the vehicle. Additionally, each LGV is provided with several manual emergency devices, like the ones indicated in Fig. 1a by 7 and 8.

A limited number of safety areas can be programmed offline on each SLS of the vehicle. They are designed depending on the plant and on the vehicle characteristics. Shapes of the safety areas can not be changed at runtime: the control system can only select, among them, the most appropriate one for each segment. The number of programmable areas is currently limited by the technology: available sensors only admit 16 safety areas. Evidently, better performances might be obtained if additional shapes were available. More in details, the limited number of programmable areas sometimes imposes using the same configurations for both tight and large bends. In the first case the vehicle speed is naturally reduced because of the kinematic limits and, consequently, safety areas are redundantly large: since tight curves are used for swift maneuvers in narrow spaces between shelves and columns, unnecessarily large safety areas could cause undesired stops. In the second case, curves could potentially be traveled at higher speeds, but the use of small areas imposes, for safety reasons, reduced velocities. In both cases the plant efficiency is penalized. Fig. 2 makes it possible to appreciate how safety areas are managed in real plants. In Fig. 2a the LGV is moving at plain speed along a straight path. In terms of safety, the frontal zone is the most critical one, so that it is protected by a very large safety area. Conversely, the rear part of the vehicle can not collide with static obstacles, so that the corresponding sensor is switched off. If the vehicle needs to execute a turn, the speed is reduced, the frontal area is scaled down accordingly, and the rear area is enlarged as shown in Fig. 2b: in fact, along turns the load sweeps laterally and may hit obstacles or coworkers. Since turns essentially imply a lateral motion, the side areas are modified as shown in Fig. 2c and the turn is finally executed (see Fig. 2d).

In industrial warehouses safety has been historically managed by means of trial-and-error approaches. Designers first define the plant layout, which is obtained through the composition of path segments, each of them being described through appropriate path primitives. Then, the same technicians assign, on the basis of their own experience, the most suitable set of safety areas to each segment. Areas are selected among the ones programmed in the SLS. Subsequently, for each segment, the most proper constant speed is selected depending on the combination between curve and safety area: it must satisfy the vehicles

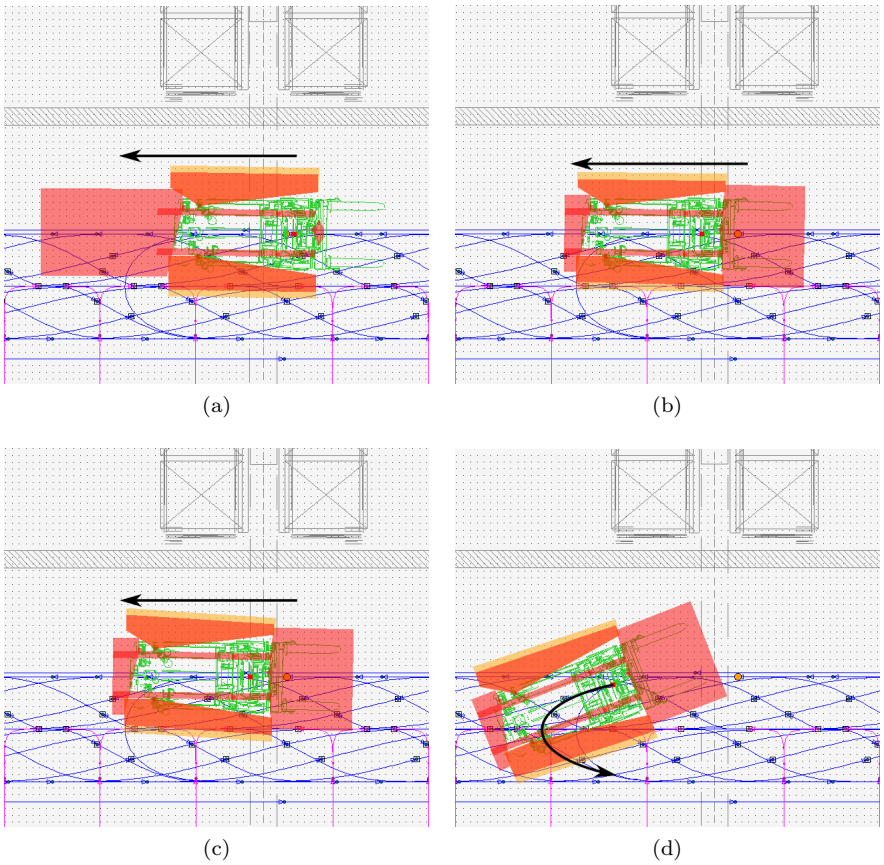

Figure 2: LGV safety areas could be modified only when the vehicle switch between two subsequent segments.

constraints and it must be safe. A single safety area and a single constant speed is assumed for each segment of the plant. Such choice is motivated by several reasons. One of them was specified in the introduction: a constant velocity reference guarantees a simplified real-time generation of the composite speed profile. Another reason is essentially practical: each plant is composed by thousand of segments, so that the manual choice, for each of them, of multiple safety areas and multiple speed references would enormously complicate the design phase.

The implementation of the system in a real plant requires a final tuning "on the field" since safety areas may be inadequate, speeds may be unfeasible, and safety conditions may be violated: they are all the result of heuristic choices. Since each segment of the plant needs to be tested, the tuning process requires long times. Previous considerations make it possible to conclude that plant performances are strongly affected by the designers experience.

The SAFERUN project aimed at the partial automation of the design pro-

cess, so as to make it more deterministic. More precisely, while plant designers still need to select curve layouts and safety areas, a smart velocity planner synthesizes, in real time, a speed reference which fulfills all the system constraints, including the safety ones. Such planner, recently proposed in [21], is explicitly suited for LGV applications and shows characteristics which are not owned by alternative algorithms. For example, well known real-time planners [26, 27, 28] consider constant bounds for velocity, acceleration, and jerk, while the problem at hand intrinsically requires the management of variable velocity bounds expressed as functions of the vehicle position along the path. Other techniques allow variable velocity bounds [29, 30], but the algorithms which can be used in real-time contexts do not account for jerk constraints. Techniques which also consider jerk limits are based on strategies – typically nonlinear programming methods – which can hardly be adopted in real-time contexts, like the one here considered, in which control boards have limited computational capabilities.

The planner proposed in [21] is based on a heuristic technique which allows reducing the evaluation times, by returning solutions which are very close to the ones provided by nonlinear algorithms for the global optimization. In many cases, the real-time planner proposes solutions which are even better than the ones obtained through nonlinear programming methods: the problem is strongly multimodal, so that algorithms for the global optimization can be easily entrapped in local minima and better solutions can be found only by means of repeated runs from random initial states.

The novel planning technique was validated in [21] by means of simulative tests. This paper extends such work by experimentally testing the proposed planning strategy. Experiments were performed, in part, in a demonstration plant and, in part, in a real warehouse by considering actual operating conditions. In particular, the second set of tests covered a period of several months. The achieved results are discussed into the next sections.

3. Experiments in the demo plant

The first experiments were executed with a commercial LGV, produced by Elettric80 and named CB16, running in the demonstration plant shown in Fig. 3. The plant was implemented in the test shed owned by the Elettric80 company. It was conceived so as to include all the curve shapes typically used in industrial warehouses and, in particular, the ones considered critical in terms of safety or efficiency. In Fig. 3, circled numbers identify the start and the end points of each curve, while the curves IDentification numbers (ID) are highlighted through different colors. Four categories of curves were considered:

- asymmetric ‘U’ curves (red segments - IDs: 1, 2 and 3);
- symmetric ‘U’ curves (brown segments - IDs: 10, 11 and 12);
- 90 degrees curves (magenta segments - IDs: 4, 5, and 6);
- ‘S’ curves (blue segments - IDs: 7, 8, and 9).

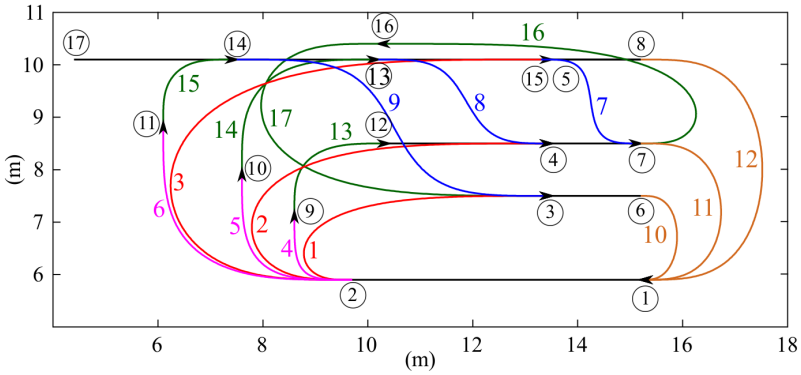

Figure 3: The demo plant used for testing the SAFERUN algorithm.

The straight segments of the plant are essentially used for single-curve tests: they are required to enter the curve at plain speed and to decelerate and stop the LGV when the curve has been executed. Plant curves were obtained through Bézier path primitives and were further classified on the basis of their maximum curvature. Three representative curvatures were selected for each category of the test set. More in details, each family includes one narrow curve, whose maximum curvature is higher than 1.7 m^{-1}, a medium one, whose curvature is in the range [0.8, 1.7] m^{-1}, and a large one, whose maximum curvature is lower than 0.8 m^{-1}. It is worth pointing out that narrow curves are seldom used in real plants because they would impose unacceptably low speeds: the experimental results proved that, conversely, the SA allows reasonable traveling times also for them.

Three types of experiments were executed. Experiment 1 was conceived so as to test the safeness of the SA velocity profiles and to show that the original SP can reach the same performances only by violating the safety conditions. Experiments 2 and 3 aimed at comparing the SA performances with the ones achieved through the SP. More precisely, Experiment 2 concerned single-curve experiments, while Experiment 3 involved composite paths.

Experiment 1 is described in Section 3.1. The comparative analysis for Experiment 2 is reported in Sections 3.2, while Section 3.3 proposes the outcomes of Experiment 3.

3.1. Experiment 1

As previously asserted, Experiment 1 tested the safeness of the SA trajectories. The same experiment also showed that collisions occur with certainty if the SP is tuned so as to achieve the same performances of the SA.

Safety tests have been carried out by placing an obstacle along the curves according to the technique described in the following. An LGV was then driven along the plant by means of the SA in order to verify that collisions were actually

avoided and that the stop distance from the obstacle were the one theoretically predicted.

The proper choice of the obstacle positions required some preliminary work, since the worst case situations had to be identified. They depend on many factors like, for example, the velocity constraint that the vehicle must fulfill. Such constraint is indicated in the following by $\tilde{v}(s)$, where s is the curvilinear coordinate which specifies the vehicle position along the segment. For a general discussion concerning the synthesis of $\tilde{v}(s)$ the interested reader can refer to [21], however some additional details regarding its practical implementation are reported in the following for completeness. As shown in [21], for each position s along the path, the control system can extrapolate a distance $\hat{d}(s)$ that can be safely traveled by avoiding collisions. Such distance depends on the path, on the vehicle shape, and on the shape of the safety area: safeness is guaranteed if the vehicle can be stopped before such distance is covered. In order to preserve a reasonable safety margin, which is added to account for potential tolerances, in real plants the safety distance is always downrated as follows

$$\tilde{d}(s) := \hat{d}(s) - \Delta d(s),$$

where

$$\Delta d(s) := \min\{d_M, a\,\hat{d}(s)\}, \quad a \in [0, 1]. \tag{1}$$

Practically, safety margin $\Delta d(s)$ is proportional to $\hat{d}(s)$ and it is superiorly saturated by d_M. The rationale of this choice is that, if $\hat{d}(s)$ is small, the vehicle speed is intrinsically kept small by the velocity planner, so that the safety margin can be reduced accordingly. For the tests, it was assumed $d_M = 0.2$ m and $a = 0.1$, which implies that the maximum safety margin was equal to 0.2 m. Both parameters can be modified depending on the plant and on the vehicle characteristics. $\tilde{v}_s(s)$ is then selected, according to the procedure described in [21], so as to guarantee that any vehicle moving at a speed $v(s) \leq \tilde{v}_s(s)$ could be stopped within a distance $\hat{d}(s) - \Delta d(s)$.

Some preliminary tests highlighted a behavior that was not originally foreseen and which required the implementation of an alternative method for the evaluation of $\tilde{d}(s)$. Alarms generated by SLSs are always "filtered" so as to avoid false positives caused by dust or reflected lights. As a consequence, an obstacle must be detected by several subsequent scans before the safety area is declared unclear. Such detection method evidently introduces a latency time Δt between the moment in which the obstacle is detected and the one in which the vehicle reacts to the emergency. The velocity upper bound used for the synthesis of the speed profile is clearly affected by such latency and, in particular, higher latencies impose lower velocity limits. During the latency time, the acceleration can be assumed constant, so that the vehicle approximately blindly covers the following distance

$$\Delta l = \dot{s}\,\Delta t + \frac{1}{2}\ddot{s}\,\Delta t^2 = v(s)\Delta t + \frac{1}{2}a(s)\Delta t^2.$$

The knowledge of Δl is clearly important because it influences the shape of $\tilde{v}(s)$. Unfortunately, $v(s)$ and $a(s)$ are computed at run time, so that they are still

unknown when $\tilde{v}(s)$ is evaluated. A rough estimate for Δl can be obtained by assuming that actual velocity profiles $v(s)$ would follow very closely $\tilde{v}(s)$. Such consideration suggested the following procedure for the synthesis of the velocity constraint:

1. initially assume $\tilde{d}(s) = \hat{d}(s)$ and tentatively evaluate $\tilde{v}(s)$ with the procedure proposed in [21];
2. evaluate:
$$\Delta l(s) = \tilde{v}(s)\Delta t + \frac{1}{2}\,\bar{a}\Delta t^2; \tag{2}$$
3. evaluate $\Delta d(s)$ according to (1) and find $\tilde{v}(s)$ by assuming $\tilde{d}(s) := \hat{d}(s) - \Delta l(s) - \Delta d(s)$.

It is worth remarking that the first term in (2) typically overestimates $\Delta l(s)$ since $\tilde{v}(s) \geq v(s)$. In the second term, $\bar{a}$ could be conservatively selected equal to the acceleration upper bound. However, the experience has shown that the overestimation introduced by the first term and the subsequent use of $\Delta d(s)$, allows one imposing $\bar{a} = 0$ in any practical case, with no impact on the safety.

The experimental tests have shown that the actual distance required for the complete stop of the vehicle in emergency situations is generally shorter than $\hat{d}(s) - \Delta d(s)$ because the optimal velocity profile evaluated through the SA is normally smaller than $\tilde{v}_s(s)$. This evidently leads to higher safety standards.

Space reasons do not allow a detailed analysis for all the curves of the demo plant. For such reason, a single curve of the test set – more precisely the second one, i.e., an asymmetric 'U' curve with a medium curvature – will be extensively discussed in the following, while a concise analysis is provided for the remaining curves of the test set.

As shown in [21], the velocity constraint is obtained by considering several contributions. More precisely, for each point s of the curve, the more stringent between the safety and the kinematic speed limits is assumed. For such reason, safety tests were only performed in path positions characterized by a safety constraint more limiting than the kinematic one: in the other points safeness is certainly verified. Fig. 4 shows the kinematic and the safety limits for the second curve expressed as function of s: for the selected curve all the points are potentially risky. The same figure reveals that seven test points were chosen. Some of them were placed in the most critical locations of the path, i.e., the ones in which the SA velocity reference (solid blue line) touches the safety constraint (dashed red line): β, χ, δ, and ϕ. The remaining points (α, ϵ, and γ) were casually placed along the path for validation reasons. The physical collocation of the obstacles was then obtained by means of simulations. For example, Fig. 5a shows the procedure followed for point α. When the vehicle crosses point α (see the blue shape), the SLSs verify if the safety area (see the red shape) is clean from obstacles and, in that case, the LGV can move up to α' (see the green shape) without collision risks: the distance between α and α' coincides with $\hat{d}(s)$. In such situation, the first point in which a collision may occur is indicated by a cross: it is the place in which the obstacle must be posed for the test concerning the α point. The same procedure was followed for all

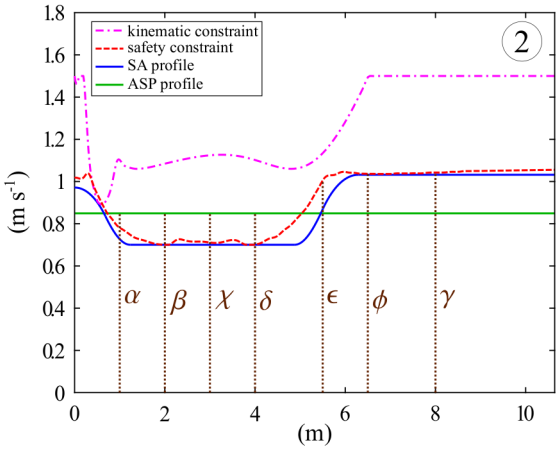

Figure 4: Velocity profile for the second curve of the demo plant. The following convention is assumed: the dash-dotted magenta line indicates the kinematic constraint; the dashed red line indicates safety constraint $\tilde{v}(s)$; the solid blue line indicates the SA optimized profile; the solid green line indicates the SP profile used to emulate the SA performances; the dotted vertical brown lines indicates the obstacles positions.

the seven test locations. Fig. 5b shows that, sometimes, more than one point needs to be tested, while Fig. 6 shows that the critical impact point may change depending on the vehicle position along the path.

The actual obstacle used for the experiments was a small carton box. The tests revealed that the SLSs reactivity is influenced by the box orientation, so that each single experiment was repeated different times by turning the box in several directions: data reported in Table 1 refer to the worst case situations detected for each one of the seven positions.

Tests were executed by first using the SA and, then, the SP. The velocity of the SP was augmented in order to obtain the same time performances of the SA. In the following, the SP with augmented speed will be synthetically referred as ASP. The first two columns of Table 1 list the distances between LGV and obstacle that were measured after an emergency stop. The last column reports the theoretical values of Δd provided by (1) for the seven test points.

A rapid inspection of the table reveals that the ASP caused collisions in configurations β, χ, and δ. Point α is critical as well: the collision was avoided only because of the safety margin Δd. Conversely, with the SA the final distance was always higher or equal to the theoretical value of Δd. The multimedia file Video1.mp4 attached to this paper visually compares the two planning techniques for the seven test points.

Table 1 can be deeply analyzed with the aid of Fig. 4:

- Configuration α: the SA profile (solid blue line) is decreasing and it is smaller than the safety constraint, so that the measured stop distance was slightly higher than Δd. On the contrary, the constant velocity assumed

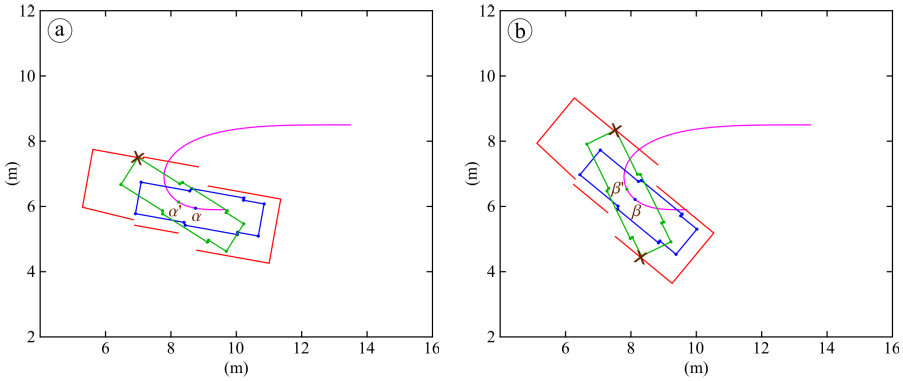

Figure 5: Most critical collision points for the α and β experiments on curve ID 2.

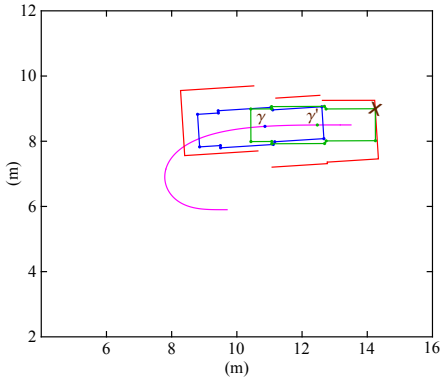

Figure 6: Most critical collision point for the γ experiment on curve ID 2.

for the ASP is slightly higher than the safe speed and, consequently, the detected stop distance was smaller than Δd. The situation is clearly unsafe: the collision was avoided thanks to the added safety margin Δd.

- Configurations β, χ, δ: the situation is similar in the three cases. The ASP profile evidently violates the safety constraint and, consequently, a collision occurred for all the three cases. Conversely, the SA speed touches the safety constraint, so that the vehicle was stopped at a distance from the obstacle that practically coincided with Δd.
- Configuration ϵ: the two planning techniques generate speeds that are much smaller than the safety constraint, hence the stopping distance from the obstacle was, in both cases, higher than Δd. A lower margin was obtained for SA since the LGV was accelerating at the time the obstacle was detected.
- Configurations ϕ, γ: the two configurations are similar. The SA speed is close to the safety constraint, so that the stop distance was similar to Δd.

Table 1: Curve ID 2: comparisons between experimental Δd obtained with SA and with the ASP. OBS indicates the obstacle identification letter, as defined in Fig. 4. A negative value indicates a collision. Δd is the theoretical stop distance obtained with (1).

OBS	**Experimental results**		Δd [m^{-2}]
	ASP [m^{-2}]	**SA** [m^{-2}]	
α	5.5	22.0	19.1
β	-1.0	14.0	13.7
χ	-3.0	13.5	12.7
δ	-1.0	15.0	13.7
ϵ	46.0	30.0	20.0
ϕ	49.0	20.0	20.0
γ	49.0	20.0	20.0

The ASP speed is much lower than the constraint, so that the LGV was stopped very far from the obstacle.

In conclusion, for the second curve of the test set the SA always guaranteed stop distances which were higher than or equal to Δd, while the ASP caused collisions due to the high speeds required to obtain the same performances.

The same experiment was replicated for the other curves of the test set. However, a single test point was placed in the most critical location of each curve. Such location coincided with a configuration in which the SA speed is very close to, or touches, the safety constraint which, in turn, is violated by the ASP (see, for example, positions β, χ, and δ of Fig. 4). The experimental results are listed in Table 2, which highlights that, in many cases, the LGV was not able to execute the ASP profile because the required velocity was too high: the path tracking was lost and the vehicle was stopped by the emergency controls.

Summarizing, the results obtained for Experiment 1 confirm the expectations. For each curve of the test set, the SA guarantees stop distances that are higher than $\Delta d(s)$, even considering multiple repetitions of the same experiment. Conversely, if the cruising speed of the SP is increased in order to achieve the same traveling times, three situations may occur: the path tracking is lost, or safety margin $\Delta d(s)$ is not satisfied or, in the worst cases, a collision occurs.

3.2. Experiment 2

Experiment 2 is a single curve performance test involving all the curves of the plant. The experiment was first simulated in the Matlab environment and, then, it was replicated in the demo plant, so as to verify if the expected figures were met. It is worth noticing, indeed, that velocity references were planned by neglecting the dynamic constraints, so that discrepancies between simulated and experimental results should have been possible. Table 3 summarizes the performances achieved for each one of the 17 curves. The second and the third columns list the simulated traveling times obtained with the SP and with the SA, respectively. Velocities for the SP coincide with the ones that would actually

Table 2: Comparison between experimental Δd obtained with the SA and with the ASP. ID indicates the curve ID. A negative value indicates a collision. Δd is the theoretical stop distance obtained through (1). "–" indicates that the speed was too high to correctly execute the curve.

ID	**Experimental results**		Δd [m^{-2}]
	ASP [m^{-2}]	**SA** [m^{-2}]	
1	–	15.0	13.6
3	-10.0	7.5	6.5
4	–	14.5	13.8
5	2.0	9.0	7.3
6	-2.0	15.0	12.7
7	–	17.0	15.2
8	–	11.5	10.3
9	2.0	17.0	16.5
10	–	13.5	11.2
11	–	13.0	12.2
12	3.0	16.0	14.9
13	–	16.0	14.8
14	9.0	20.5	20.0
15	–	11.5	10.0
16	–	12.5	11.6
17	9.5	23.0	20.0

be used during normal operations, i.e., they are all feasible with respect to the constraints. Traveling times do not include the launch and the stop segments, i.e., they only refer to the execution of the test curves. The expected percentage time-gains are shown in the fourth column and are defined as follows

$$\text{Gain} := \frac{t_{SP} - t_{SA}}{t_{SP}} \cdot 100,$$

where t_{SP} and t_{SA} are the travelling times achieved with the SP and the SA, respectively.

Columns from 5 to 7 report the analogous figures acquired in the demo plant with the test vehicle. They are directly obtained from the LGV log files.

Simulated and actual performances are quite similar. The average time-gain, obtained by considering the whole set of curves, was equal to 31.17%, i.e., it was very close to the figure obtained through simulations, which was equal to 31.68%. It is important to point out that such result was achieved despite the reference speed of the actual vehicle may be influenced by components of the control system which were not simulated.

Fig. 7 allows to visually compare the results obtained for the second curve. Simulated and actual speeds are indistinguishable for the SP, while for the SA some small differences can be noticed. They are due to some LGV control algorithms that were not simulated and which slightly modify the velocity ref-

Table 3: Comparison between simulated and experimental results. ID is the curve identification number (see also Fig. 3).

ID	Simulation results			Experimental results		
	SP (s)	SA (s)	Gain (%)	SP (s)	SA (s)	Gain (%)
1	33.26	13.23	60.23	33.46	13.39	59.98
2	15.20	12.53	17.56	15.33	12.68	17.27
3	17.84	14.09	21.01	18.07	14.27	21.00
4	9.55	6.78	28.99	9.60	6.92	27.93
5	6.48	5.55	14.38	6.52	5.61	13.98
6	9.25	7.23	21.82	9.35	7.38	21.04
7	20.25	12.19	39.83	20.62	12.54	39.17
8	13.50	9.22	31.68	13.67	9.49	30.55
9	11.15	9.56	14.28	11.33	9.78	13.70
10	59.67	11.94	79.98	60.66	11.87	80.43
11	15.02	10.32	31.30	15.09	10.4	30.98
12	12.83	10.99	14.32	12.90	11.11	13.89
13	11.11	6.28	43.47	11.27	6.47	42.56
14	7.65	6.55	14.42	7.71	6.67	13.49
15	10.81	6.80	37.09	10.89	6.97	36.03
16	31.06	14.87	52.11	31.48	15.11	52.01
17	15.11	12.69	16.04	15.32	12.88	15.85

erence in order to accomplish some secondary tasks. As previously stated, they minimally affect traveling times, as proved by Table 3.

Fig. 7 also shows that velocity constraint $\widetilde{v}(s)$ is always strictly satisfied so that the safety requirement, as well as the kinematic constraints, are both fulfilled. Similar figures were obtained for all the curves of the test set.

The algorithms performances are visually compared in the second multimedia attachment, named Video2.mp4, which refers to curve 1, i.e., an asymmetric 'U' turn with high curvature. The time-gain is evident and proves that the SA allows tracking very tight curves by simultaneously preventing efficiency losses.

3.3. Experiment 3

The last set of experiments was relative to the execution of 5 composite paths and to the acquisition of the corresponding traveling times. The plant layout is still the same of Fig. 3. The sequences of via-points adopted for each one of the composite paths are listed in Table 4.

The results achieved for Path 1 are summarized in Table 5, which columns are organized similarly to the ones of Table 3. A good agreement between simulated and experimental results has been verified. As expected, the highest time-gains are detected for the segments with the highest curvatures, but the SA also allowed consistent time savings during the execution of straight segments. In fact, vehicles driven with the SA enter and leave curvilinear paths at higher

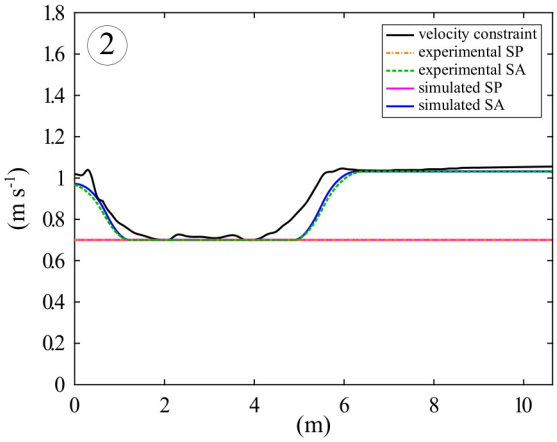

Figure 7: Asymmetric 'U' curve: comparisons between the simulated and the actual velocity functions obtained with the SP and with the SA algorithms. A solid black line is used for the kinematic and safety constraint function $\tilde{v}(s)$; a dash-dotted orange line is used for the experimental (LGV log files) SP velocity function; a dashed green line is used for the experimental (LGV log files) SA velocity function; a solid magenta line is used for the simulated SP velocity function; a solid blue line is used for the simulated SA velocity function.

Table 4: The sequence of via-points for the 5 composite paths used in Experiment 3.

Path 1	$1 \rightarrow 2 \rightarrow 9 \rightarrow 12 \rightarrow 7 \rightarrow 1 \rightarrow 2 \rightarrow 4$
Path 2	$17 \rightarrow 8 \rightarrow 1 \rightarrow 2 \rightarrow 10 \rightarrow 13 \rightarrow 15 \rightarrow 7 \rightarrow 1$
Path 3	$17 \rightarrow 14 \rightarrow 3 \rightarrow 6 \rightarrow 1 \rightarrow 2 \rightarrow 11 \rightarrow 14$
Path 4	$1 \rightarrow 2 \rightarrow 5 \rightarrow 8 \rightarrow 1 \rightarrow 2 \rightarrow 3 \rightarrow 6$
Path 5	$17 \rightarrow 13 \rightarrow 4 \rightarrow 7 \rightarrow 16 \rightarrow 3 \rightarrow 6$

speeds and, consequently, straight segments following or preceding such curves are executed in less time.

System performances can also be visually compared by means of Fig. 8. The SA velocities are everywhere higher than the SP ones, apart from the positions in which the SA profile coincides with the constraint minima. More evident improvements were achieved for curvilinear segments (the 2nd, the 3rd, the 5th, and the 7th), although time-gains were also detected for straight paths (the 1st, the 4th, and the 6th).

Simulated and experimental profiles are almost identical and differences, like in Experiment 2, are essentially due to controller behaviors that were not modeled. For example, in the highlighted detail, relative to the last curve of the composite path, the two references differ: every time the vehicle is stopped, the velocity function is automatically downscaled by the control system in order to approach the end-point at a very low speed. This guarantees a more accurate final positioning, but it prolongs traveling times.

For space reasons, the visual analysis for the other four composite paths is omitted, but similar considerations could be drawn. Conversely, the numerical

Table 5: Comparison between simulated and experimental results for each segment of composite Path 1. ID identifies the via points of the composite path (see also Fig. 3).

ID	Simulation results			Experimental results		
	SP (s)	SA (s)	Gain (%)	SP (s)	SA (s)	Gain (%)
1 → 2	7.37	7.16	2.92	8.23	8.00	2.77
2 → 9	9.57	7.07	26.12	9.58	7.12	25.67
9 → 12	11.11	6.32	43.11	11.26	6.47	42.58
12 → 7	5.90	4.92	16.64	6.20	5.18	16.52
7 → 1	15.02	10.32	31.30	15.10	10.41	31.05
1 → 2	5.67	5.29	6.82	5.94	5.53	6.81
2 → 4	16.47	14.22	13.68	19.05	17.16	9.89

Table 6: Comparison between simulated and experimental results. ID is the path identification number.

ID	Simulation results			Experimental results		
	SP (s)	SA (s)	Gain (%)	SP (s)	SA (s)	Gain (%)
1	71.11	55.29	22.26	75.36	59.88	20.55
2	83.31	64.99	22.00	86.45	67.47	21.96
3	106.93	50.73	52.53	110.77	53.76	51.47
4	83.05	55.29	33.43	87.00	59.55	31.55
5	74.48	50.66	31.98	79.02	55.20	30.15

analysis for the 5 composite paths is proposed in Table 6. Average time-gains are quite different depending on the path composition. Higher gains are typical for routes obtained by composing many narrow curves with a minor number of straight segments.

The cumulative time-gain measured for the 5 composite paths was equal to 31.13%. It was very close to the simulated figure that was equal to 32.44%.

4. Experiments in an actual warehouse under real operative conditions

The tests proposed in Section 3 were relative to an ideal situation concerning a single LGV traveling along the routes of an empty plant. Under actual operating conditions, the plant is shared among several vehicles and also with human operators, so that traffic problems may arise and lower time gains have to be expected.

For such reason, an extensive test campaign was executed in a real warehouse by considering actual operating conditions. The selected plant currently uses five LGVs subdivided into two categories: two model CB12 vehicles and three model LT3 vehicles. Both LGVs are shown in Fig. 9. The CB12 vehicles were equipped with the SA, while the LT3 machines were driven with the SP. The

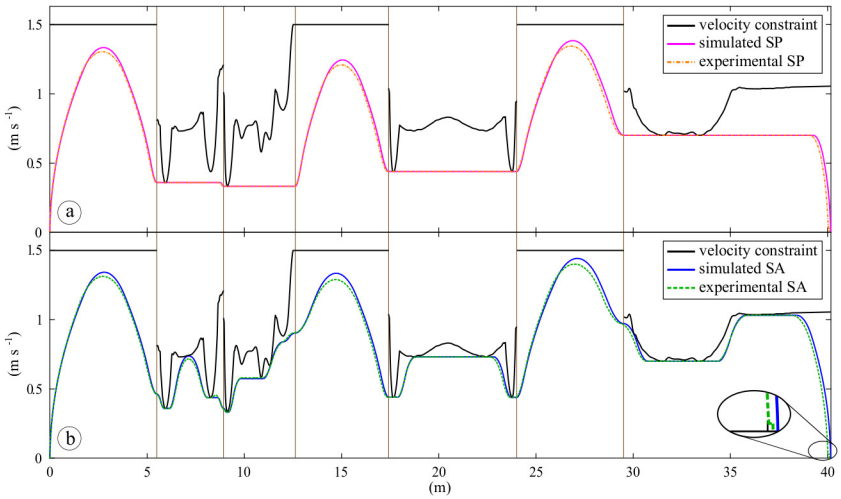

Figure 8: Comparison between simulated and experimental results for Path 1, obtained for (a) the SP and (b) the SA. The vertical brown lines separate the different segments of the composite path, while black solid lines are used for the velocity constraint. In (a) a solid magenta line is used for the simulated results, while a dash-dotted orange line is used for the experimental data. In (b) a solid blue line is used for the simulated results, while a dashed green line is used for the experimental data.

reason of such choice can be understood with the aid of Fig. 10, which shows the plant layouts for the two classes of vehicles. Working areas are clearly different, although some zones are shared. The CB12 vehicles are mainly used to transfer goods between different locations of the plant. Conversely, the LT3 vehicles are principally used to store pallets, so that they mainly operate within shelves: their paths are essential straight segments. As early pointed out, the SA allows marginal time improvements for straight segments, so that upgrade costs were not justified for LT3 vehicles.

The SA was preliminary tested in the warehouse by executing some selected composite paths, in order to verify its reliability. Video3.mp4 visually compares the performances achieved with the SA and with the SP for one of the chosen paths. Additional videos concerning other composite paths can be found in [31].

After such initial tuning phase, the SA was used to drive the two upgraded vehicles during the warehouse daily operations. The performance comparisons proposed in the next subsections are based on the log data collected in the period from May to November 2016, i.e., when all LGVs were still driven by the SP, and the ones acquired in the period from September to November 2017, i.e., after the implementation of the SA. The results of Section 4.1 refer to the performances of the sole CB12 vehicles, while the ones in Section 4.2 extend the comparisons to all the plant vehicles.

Owing to the high number of curves, safety tests only involved the most critical segments, i.e., the ones with high curvatures, plus a set of randomly

(a) *Model CB12 vehicle* (b) *Model LT3 vehicle*

Figure 9: The two LGV models used in the industrial plant considered. (Courtesy of Elettric80).

selected paths. The obtained results were perfectly congruent with the ones reported in Section 3.1 and, for this reason, they are not discussed.

4.1. Statistics concerning the CB12 vehicles

In real plants, like the warehouse here considered, LGVs missions change continuously, so that the performance analysis can not consider repetitive travels. For such reasons, missions were preliminarily classified depending on the travel typology. To this purpose, the vehicles docking stations were first grouped depending on their function. The warehouse used for the experiment has an entry area where raw materials are unloaded from trucks and an exit area used to load the final product on the trucks. Perishable materials are stored into a cooled region, while remaining materials are stored into standard shelf units. Pallets are also moved from the storing sections to the production area and viceversa. Such working organization suggested the following grouping scheme for the docking stations (the number of stations associated to each functionality is indicated within brackets):

- Truck unload stations (6)
- Production stations (3)
- Fridge entrance stations (2)

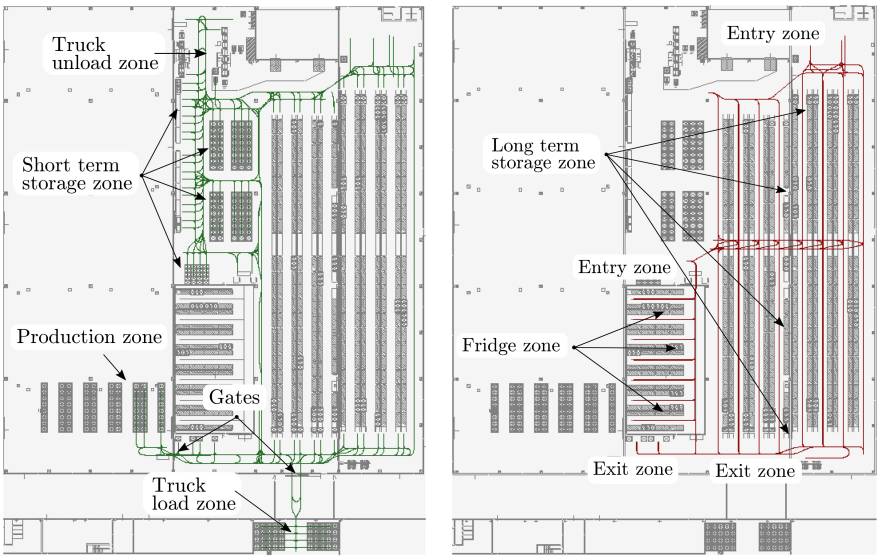

(a) (b)

Figure 10: Plant layouts for the CB12 vehicles (a) and for the LT3 vehicles (b).

- Fridge exit stations (4)
- Short term storage stations (32 – actually used: 10)
- Entry points for long term storage stations (15)
- Exit points for long term storage stations (14)
- Truck load stations (8)

The statistical study has been carried out by considering travels involving homogeneous working conditions. In particular, travels were grouped into the following four categories:

1. from the "Truck unload stations" to the "Fridge entry stations", or to the "Short term storage stations", or to the "Entry stations for long term storage zone" (see Fig. 11a);
2. from the "Truck unload stations" or from the "Short term storage stations" to the "Production stations" (see Fig. 11b);
3. from the "Fridge exit stations" or from the "Exit stations from long term storage zone" to the "Production stations" (see Fig. 12a);
4. from the "Production stations" or from the "Exit stations from long term storage zone" to the "Truck load stations" (see Fig. 12b).

Statistics were acquired for each travel category. Table 7 reports the comparative results. In particular it contains, for each class of travel, the following data:

- number of station-to-station missions;

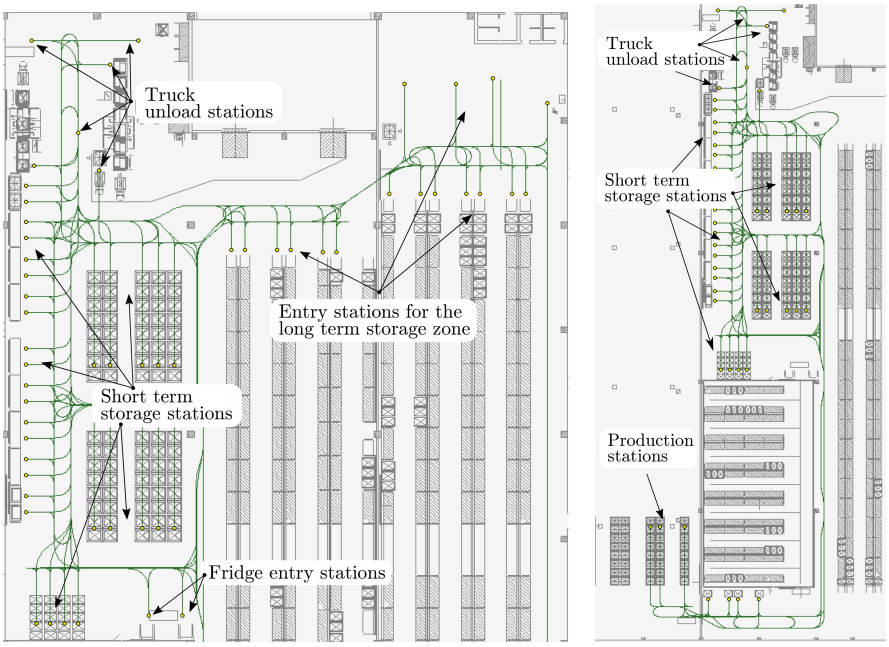

(a) Paths from the truck unload stations to fridge entry, to the long term entry, and to short term storage stations.

(b) Paths from the truck unload stations and from the short term storage stations to the production stations.

Figure 11: Travel categories 1 (a) and 2 (b).

- the average mission times;
- the resulting time-gains.

Time-gains in Table 7 evidently depend on the travel category. For example, missions of categories 2, 3 and 4 pass through (at least) one normally closed gate. The time required to open the gate imposes a stop to the LGV and, consequently, the SA does not operate for long periods: any stop – especially long ones – affects negatively the statistics, since average mission-times increase and percentage time-gains necessarily decrease. The most critical situations occur for the paths of category 4, since they often require crossing two gates.

Mission times are also affected by the LGV backward movements required to approach a load/unload station. Backward movements worsen the average performances, since they impose an additional stop in order to revert the motion direction and, furthermore, they require a point-to-point movement executed at a very low speed ($0.3\ \mathrm{ms}^{-1}$ according to the "EN ISO 1525:1997"), during which the SA does not operate.

The plant traffic can be more or less invasive depending on the mission category and, consequently, its effect on the statistics may be different. Traffic

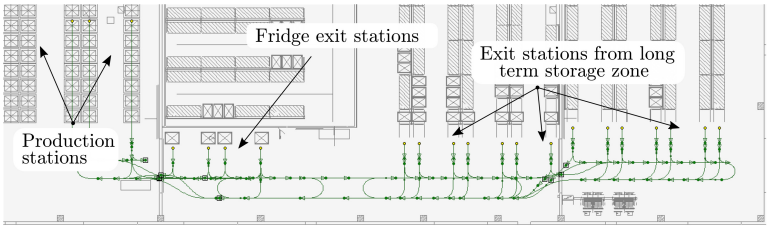

(a) Paths from fridge exit stations and from the long term exit stations to the production stations.

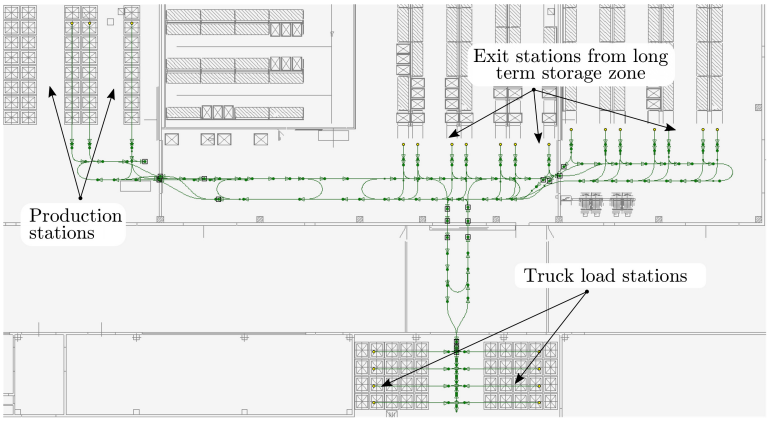

(b) Paths from the production stations and from the long term exit stations to the truck load stations.

Figure 12: Travel categories 3 (a) and 4 (b).

stops may be caused by human operators or by the interaction with other LGVs. For example, category 2 missions intersect the LT3 paths in many points, so that CB12 vehicles are stopped very frequently.

Finally, the SA performances depend on the number of straight segments of each mission: improvements are essentially expected for curvilinear segments.

The average traveling time, evaluated over the entire set of missions, was equal to 121.41 s for the SP, while it reduced to 111.11 s when the SA was adopted. The average time-gain for the two CB12 vehicles, obtained by considering a weighting factor which depends on the number of travels, was equal to 8.48%.

4.2. Statistics concerning all the vehicles

The SA installed on the CB12 vehicles has a positive influence also on the performances of the LT3 vehicles which still use the SP. A short analysis is proposed in the following in order to quantify the cumulative effects on the plant efficiency. The same statistical analysis proposed in Section 4.1 has been repeated by also considering the performances of the LT3 machines, i.e., the ones that were not upgraded. Table 8 reports the results acquired for the two

Table 7: Performance comparisons involving the CB12 vehicles.

Category	Number of missions		Average times		Gain (%)
	2016	2017	2016 (s)	2017 (s)	
1	4862	1827	113.63	101.41	10.71
2	798	254	164.06	161.87	1.33
3	1976	471	118.72	109.64	7.65
4	893	284	131.56	130.12	1.09

Table 8: Performance comparisons involving both the CB12 and the LT3 vehicles.

LGV type	Number of missions		Average times		Gain (%)
	2016	2017	2016 (s)	2017 (s)	
LT3	8095	2639	157.91	156.28	1.03
CB12	8529	2836	121.41	111.11	8.48

classes of LGVs. It is worth noticing that a small time-gain was detected also for the LT3 vehicles: they found more frequently an empty route, so that traveling times reduced accordingly.

The statistical analysis has been finally repeated by simultaneously considering all the five LGVs. The average traveling time, measured when all vehicles were driven through the SP, was equal to 139.18 s. Conversely, in the period from September to November 2017, the average traveling time decreased to 132.88 s. As a consequence, for the considered plant and time periods, the SA allowed a weighted, omni-comprehensive time-gain equal to 4.53%. This result was achieved despite only two vehicles were upgraded over the five used in the plant. Since the working conditions in the two test periods were exactly the same and no further changes were introduced in the plant, it can be asserted that efficiency improvements were only due to the SAFERUN Algorithm.

5. Conclusions

The paper reported the experimental validation of a recently proposed safe velocity planner for LGV based plants. In particular, the main planner characteristic is that it can analytically handle safety concerns which were early managed through a trial-and-error approach.

The experimental results, reported in this paper, highlight performances which are very close to the expected ones. This is very important since it implies that good predictions of the plant behavior can be achieved through the execution of preliminary simulations.

The experiments were not limited to laboratory tests but, conversely, they also concerned a significant validation period in a industrial plant, under real operative conditions. During such period, which lasted three months, the planner proved its reliability.

The average time-gain measured under real operating conditions – and consequently accounting for the plant non-idealities – was equal, for the upgraded vehicles, to 8.48%. Such figure is very important since it refers to a plant with a limited traffic and with a high number of straight segments: achievable gains may be higher for plants with a larger number of vehicles and with more complex layouts. Since the performance improvements were evident, the SA was maintained active after the conclusion of the experimental phase and it is still used to drive the plant. The interested reader can refer to [31] for a complete story of the SAFERUN project.

Summarizing, the SA represents an important step toward the complete automation of the design phase for LGV based plants. Next steps will concern the automatic selection of curves and safety areas, which will be chosen so as to increase the plant efficiency while preserving safe operating conditions.

Acknowledgment

This work was supported in part by the European Project ECHORD++ (The European Coordination Hub for Open Robotics Development) financed in the framework of the FP7 EU program.

Authors would like to thank the Elettric80 staff for its profitable support during the whole SAFERUN project. In particular, this work would have been impossible without the aid of the many technicians who actively collaborated for the implementation of the system in the Elettric80 facility and in the warehouse used for the tests. A special thanks goes to Eng. Francesco De Mola and Eng. Domenico Di Terlizzi for their useful advices.

References

[1] H. Martnez-Barber, D. Herrero-Prez, Autonomous navigation of an automated guided vehicle in industrial environments, Robotics and Computer-Integrated Manufacturing 26 (4) (2010) 296 – 311. doi:https://doi.org/10.1016/j.rcim.2009.10.003.
URL http://www.sciencedirect.com/science/article/pii/S0736584509000994

[2] H. Li, A. V. Savkin, An algorithm for safe navigation of mobile robots by a sensor network in dynamic cluttered industrial environments, Robotics and Computer-Integrated Manufacturing 54 (2018) 65 – 82. doi:https://doi.org/10.1016/j.rcim.2018.05.008.
URL http://www.sciencedirect.com/science/article/pii/S0736584517300844

[3] S.-Y. Lee, H.-W. Yang, Navigation of automated guided vehicles using magnet spot guidance method, Robotics and Computer-Integrated Manufacturing 28 (3) (2012) 425 – 436. doi:https://doi.org/10.1016/j.rcim.2011.11.005.

URL http://www.sciencedirect.com/science/article/pii/S0736584511001372

[4] J. Corrales, F. Candelas, F. Torres, Safe humanrobot interaction based on dynamic sphere-swept line bounding volumes, Robotics and Computer-Integrated Manufacturing 27 (1) (2011) 177 – 185. doi:https://doi.org/10.1016/j.rcim.2010.07.005.
URL http://www.sciencedirect.com/science/article/pii/S0736584510000840

[5] R. Meziane, M. J. Otis, H. Ezzaidi, Human-robot collaboration while sharing production activities in dynamic environment: Spader system, Robotics and Computer-Integrated Manufacturing 48 (2017) 243 – 253. doi:https://doi.org/10.1016/j.rcim.2017.04.010.
URL http://www.sciencedirect.com/science/article/pii/S0736584515301447

[6] T. Fraichard, A Short Paper about Motion Safety, in: IEEE Int. Conf. Robot. and Autom., ICRA07, 2007, pp. 1140–1145. doi:10.1109/ROBOT.2007.363138.

[7] P. Fiorini, Z. Shiller, Motion planning in dynamic environments using velocity obstacles, Int J. Robot. Res. 17 (7) (1998) 760–772.

[8] B. Kluge, E. Prassler, Reflective navigation: individual behaviors and group behaviors, in: IEEE Int. Conf. Robot. and Autom. (ICRA04), Vol. 4, 2004, pp. 4172–4177. doi:10.1109/ROBOT.2004.1308926.

[9] J. Van den Berg, M. Lin, D. Manocha, Reciprocal velocity obstacles for real-time multi-agent navigation, in: IEEE Int. Conf. Robot. and Autom. (ICRA08), 2008, pp. 1928–1935. doi:10.1109/ROBOT.2008.4543489.

[10] T. Fraichard, H. Asama, Inevitable collision states. A step towards safer robots?, in: IEEE/RSJ Int. Conf. Intell. Robots and Syst., IROS03, Vol. 1, 2003, pp. 388–393 vol.1. doi:10.1109/IROS.2003.1250659.

[11] L. Martinez-Gomez, T. Fraichard, An efficient and generic 2d inevitable collision state-checker, in: IEEE/RSJ Int. Conf. Intell. Robots and Syst., IROS08, 2008, pp. 234–241. doi:10.1109/IROS.2008.4650640.

[12] G. Savino, F. Giovannini, M. Fitzharris, M. Pierini, Inevitable collision states for motorcycle-to-car collision scenarios, IEEE Trans. Intell. Transp. Syst. 17 (9) (2016) 2563–2573. doi:10.1109/TITS.2016.2520084.

[13] K. Kant, S. Zucker, Toward efficient trajectory planning: The path-velocity decomposition, Int. J. Robot. Res. 5 (3) (1986) 72–89.

[14] T. Fraichard, C. Laugier, Path-velocity decomposition revisited and applied to dynamic trajectory planning, in: IEEE Int. Conf. Robot. and Autom., ICRA93, Vol. 2, Los Alamitos, CA, 1993, pp. 40–45. doi:10.1109/ROBOT.1993.292121.

[15] V. Muñoz, A. Ollero, M. Prado, A. Simón, Mobile robot trajectory planning with dynamic and kinematic constraints, in: IEEE Int. Conf. Robot. and Autom., ICRA94, Vol. 4, San Diego, CA, 1994, pp. 2802–2807.

[16] Y. Guo, L. Parker, A distributed and optimal motion planning approach for multiple mobile robots, in: IEEE Int. Conf. on Robotics & Automation, (ICRA02), Vol. 3, Washington, DC, 2002, pp. 2612–2619. doi:10.1109/ROBOT.2002.1013625.

[17] L. Huang, Velocity planning for a mobile robot to track a moving target a potential field approach, Robotics and Autonomous Systems 57 (1) (2009) 55–63. doi:https://doi.org/10.1016/j.robot.2008.02.005.

[18] G. Mahler, A. Vahidi, An optimal velocity-planning scheme for vehicle energy efficiency through probabilistic prediction of traffic-signal timing, IEEE Trans. Intell. Transp. Syst. 15 (6) (2014) 2516–2523. doi:10.1109/TITS.2014.2319306.

[19] F. Cabassi, L. Consolini, M. Locatelli, Time-optimal velocity planning by a bound-tightening technique, Computational Optimization and Applications 70 (1) (2018) 61–90. doi:10.1007/s10589-017-9978-6.
URL https://doi.org/10.1007/s10589-017-9978-6

[20] L. Biagiotti, C. Melchiorri, Trajectory planning for automatic machines and robots, Springer, Berlin, Heidelberg, Germany, 2008.

[21] M. Raineri, S. Perri, C. Guarino Lo Bianco, Online velocity planner for Laser Guided Vehicles subject to safety constraints, in: IEEE/RSJ Int. Conf. Intell. Robots and Syst., (IROS17), 2017, pp. 6178–6184. doi:10.1109/IROS.2017.8206519.

[22] Safety Standard for Driverless, Automatic Guided Vehicles and Automated Functions of Manned Industrial Vehicles, Standard ANSI/ITSDF B56.5-2012, Industrial Truck Standards Development Foundation (2012).

[23] Safety of Industrial Trucks - Driverless Trucks And Their Systems, Standard ISO 1525:1997, International Standards Organization (Sept 1997).

[24] Safety of Industrial Trucks - Additional Requirements for Automated Functions on Trucks, Standard ISO 1526:1997+A1:2008 (E), International Standards Organization (July 2008).

[25] Standard Test Method for Grid-Video Obstacle Measurement, Standard ASTM F3265-17, ASTM International, West Conshohocken, PA (2017). doi:10.1520/F3265-17.

[26] R. Haschke, E. Weitnauer, H. Ritter, On-line planning of timeoptimal, jerk-limited trajectories, in: IEEE/RSJ Int. Conf. Intell. Robots and Syst., IROS08, 2008, pp. 3248–3253. doi:10.1109/IROS.2008.4650924.

[27] X. Broquère, D. Sidobre, I. Herrera-Aguilar, Soft motion trajectory planner for service manipulator robot, in: IEEE/RSJ Int. Conf. Intell. Robots and Syst., IROS 08, 2008, pp. 2808–2813. doi:10.1109/IROS.2008.4650608.

[28] T. Kröger, F. M. Wahl, On-line trajectory generation: basic concepts for instantaneous reactions to unforeseen events, IEEE Trans. on Rob. 26 (1) (2010) 94–111. doi:10.1109/TRO.2009.2035744.

[29] K. G. Shin, N. D. McKay, Minimum-time control of robotic manipulators with geometric path constraints, IEEE Transactions on Automatic Control 30 (6) (1985) 531–541.

[30] J. E. Bobrow, S. Dubowsky, J. S. Gibson, Time-optimal control of robotics manipulators along specified paths, Int. J. Robot. Res. 4 (3) (1985) 3–17.

[31] M. Raineri, C. Guarino Lo Bianco, The SAFERUN project, http://www.ce.unipr.it/saferun/.